

# Model-based adaptive filtering of harmonic perturbations applied to high-frequency noninvasive valvometry<sup>\*</sup>

Nelson F. Barroso<sup>\*</sup> Rosane Ushirobira<sup>\*</sup> Denis Efimov<sup>\*</sup>  
Mohamedou Sow<sup>\*\*,\*\*\*</sup> Jean-Charles Massabuau<sup>\*\*\*,\*\*</sup>

<sup>\*</sup> *Inria, Univ. Lille, CNRS, UMR 9189 - CRISTAL, F-59000 Lille, France (e-mails: nelson.de-figueiredo-barroso, rosane.ushirobira, denis.efimov@inria.fr).*

<sup>\*\*</sup> *Univ. Bordeaux, EPOC, UMR 5805, F-33120 Arcachon, France.*

<sup>\*\*\*</sup> *CNRS, EPOC, UMR 5805, F-33120 Arcachon, France (e-mails: mohamedou.sow, jean-charles.massabuau@u-bordeaux.fr).*

---

**Abstract:** In this paper, a model-based adaptive filter is used to suppress electrical noise in a high-frequency noninvasive valvometry device, which is part of an autonomous biosensor system using bivalve mollusks valve-activity measurements for ecological monitoring purposes. The proposed model-based adaptive filter uses the dynamic regressor extension and mixing method to allow a decoupled estimation of the parameters. Once the desired regression form of the output model is obtained, a fixed-time estimation approach is used to identify its parameters. By applying these two techniques, a flexible filter structure is obtained with the property of retaining the major relevant components of interest of the original valve-activity signals, even in the case when the unwanted signal frequency components are in the same frequency range as the useful variables.

*Keywords:* Adaptive filtering, Fault detection, Parameter identification, Biosensors, Ecological monitoring.

---

## 1. INTRODUCTION

The appearance of noise is a common problem in the field of signal processing. Noises can originate from different sources and can also be generated anywhere in the data acquisition system, from the most fundamental level (at the sensor) to the highest level (at the data processing algorithms). Even with hardware preprocessing, it is common to post-process the signal so that it is finally ready for analysis. An important and usual step in this direction is the filtering process, used to suppress unwanted components or characteristics of a signal (Lathi, 2009).

Nowadays, to protect more effectively the marine environment across the world is an absolute priority. Recently, a generation of environmental sensors appeared in multiple labs, producing a huge amount of data, and also significant number of errors needing to be addressed. Such dataset with parasite noise are at the origin of the present work.

Conventional filters are linear blocks used in many electronic systems for anti-aliasing, signal reconstruction, and noise rejection, to name a few applications. For noise rejection, these devices are designed according to pre-defined performances in terms of the specific signal frequency ranges of interest to maintain or suppress (Lutavac et al., 2000). It is a very powerful tool widely used in the appli-

cation, however it also has some drawbacks. For example, a phenomenon that is rich in different frequencies can be excessively filtered if unwanted components are in the same signal frequency range as the frequencies considered important of the original signal, which may result in a loss of relevant information (Ljung, 1999; Pintelon and Schoukens, 2012).

Conversely, adaptive algorithms use an input vector and the desired performance specification, selected accordingly to the application, to calculate an estimated error. This error is used to adjust the filter coefficients, giving rise to a system with a more flexible structure. The two schemes most commonly used for adaptive filters are the finite impulse response (FIR) and infinite impulse response (IIR) that come naturally from the classical linear approach (Widrow and Stearns, 1985). However, as a consequence of implemented online tuning algorithms in which parameters are adjusted using input/output data, these systems become nonlinear devices and the advantages of adaptation bring costs such as a large number of parameters or stability issues.

Instead of using such adaptive devices, it is possible to propose a model for the original signal and to estimate its parameters using an appropriate estimation algorithm. In this case, a filter problem becomes a parameter estimation problem for an output model in which unwanted components are indirectly included by means of failure models and the filtered response is provided by means of estimated

---

<sup>\*</sup> This work was supported by the ANR project WaQMoS (ANR 15 CE 04 0002). Nelson F. Barroso is partly supported by the regional council of Hauts-de-France.

output in the absence of these faulty components. Such an approach comes from the fault diagnosis theory (Gao et al., 2015) and its advantage is that relevant information from the original signal is retained regardless of unwanted components in the same frequency range.

In this note an adaptive model-based filtering algorithm is designed to cancel the influence of an electrical noise in a high-frequency noninvasive valvometry system installed in an Arctic region. The Arctic region is chosen mainly by its sensitivity to climatic and environmental variations. Due to severe environmental conditions and the desired autonomy of the system for a long period without human intervention, the system must be robust and tolerant in the presence of electrical problems and electronic noise. Unfortunately, these faults are hardly avoidable, and the main issue occurs when both frequency spectrum of the electronic perturbations and the useful signal coincide. In this case, it is required to design a filtering algorithm that recovers the useful information as much as possible and clear the noise consequences<sup>1</sup>.

The outline of this paper is as follows. The experimental setup description and the problem statement are introduced in Section 2. Section 3 presents preliminaries used in the main results, which are formulated in Section 4. Concluding discussion is given in Section 5.

## 2. DATA ACQUISITION SYSTEM DESCRIPTION AND PROBLEM STATEMENT

The high-frequency noninvasive (HFNI) valvometer is an essential part of a biosensor monitoring system employed to monitor the valve opening/closing activity of bivalve mollusks (Andrade et al., 2016). The system allows the online study of their behavior in their natural habitat without significant interference. Another considerable advantage is that the system is completely autonomous without *in situ* human intervention for at least one full year.

In a typical field deployment, the system is composed of 16 animals, each one equipped with two lightweight coils (sensors) fixed on the edge of each valve (Fig. 1a). One of the coils emits a high-frequency sinusoidal signal, that is received by the second one. The strength of the electric field produced between the two coils is proportional to the inverse of the distance between them which allows to characterize the relative opening/closing valve activity. Normally, the distance measurements are scaled between 0 and 1 for completely closed and opened respectively. The measurements are performed every 0.1 seconds successively (with the frequency equal to  $\frac{10Hz}{16}$  for each of the sixteen animals). This means that the behavior of a particular animal is measured every 1.6 seconds. Every day, 54000 triplets (1 animal number, 1 distance, and 1 stamped time value) are collected for each animal.

The first level of the data acquisition system is an analog electronic card immersed in the sea close to the animals (Fig. 1b). This module is protected by a waterproof case and manages the measured signals from the sensors sending them to a second level electronic card held on the sea surface or located on land (Fig. 1c). This second

<sup>1</sup> Due to difficulties of installation and maintenance of the equipment in Arctic, all measured information is rather important.

module by its turn is equipped with a GSM/GPRS modem and uses a Linux operating system for driving the first control module immersed in the water, managing the data and meta-data storage, including timestamp, accessing the internet, and transferring the data to a central workstation server (Master Unit), located in the marine station at Arcachon (France) where the valve-activity data is finally stored in a central database (Fig. 1d), daily processed and analyzed. More details about the HFNI valvometer can be found at the *MolluSCAN eye* website (<https://molluscan-eye.epoc.u-bordeaux.fr>) and in Andrade et al. (2016).

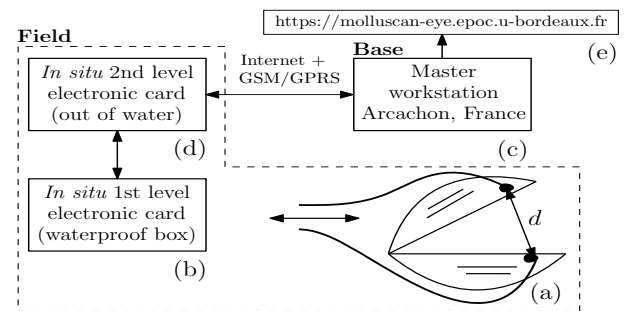


Fig. 1. Schematic representation of the HFNI valvometer

In this paper, we are interested in filtering an electrical noise that appears in the data of valve opening/closing activity signals of scallops *Chlamys islandica* (identified by numbers from #1 to #16) acquired in 2017 by using the HFNI valvometer. The monitoring site is located in Ny-Alesund, Svalbard (Norway, latitude: 11° 54' 36" E, longitude: 78° 54' 36" N). A sampling window of such signal for the animal #1 is shown in Fig. 2 where the time axis is in hours base counted from the first day of 2017. The window refers to the data collected from the day 320 at 00h00min to the day 321 at 12h00min. It is noted that the main behavior of the signal is marked by the presence of almost periodic events (highlighted in this record) occurring with a period around 4.4 hours.

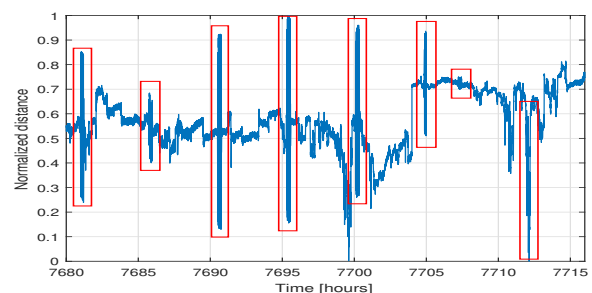


Fig. 2. A sampling window of the distance signal measured from animal #1 from the day 320 to 321.5 in 2017

In Fig. 3 an example of these events is shown in a zoomed way and, it appears as a periodic oscillation lasting approximately 0.3 hours with a relatively well defined shape, typical of an electronic noise without biological meaning. The same kind of noise also was detected in the signals measured from the others 15 individuals. Our goal was to suppress this noise from the measured signal at the server level by applying a post-processing algorithm.

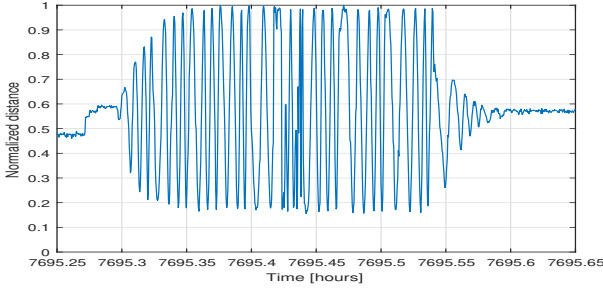


Fig. 3. Presumed electronic noise shape in the distance signal measured from the animal #1 in 2017

### 3. PRELIMINARIES

#### Notation

- Let  $\mathbb{R}_+ = \{x \in \mathbb{R} : x \geq 0\}$ . Denote by  $|x|$  the absolute value for  $x \in \mathbb{R}$  or a vector norm for  $x \in \mathbb{R}^n$ .
- For a Lebesgue measurable and essentially bounded function  $x : \mathbb{R} \rightarrow \mathbb{R}$  denote  $\|x\|_\infty = \text{ess sup}_{t \in \mathbb{R}} |x(t)|$ , and define by  $\mathcal{L}_\infty(\mathbb{R}, \mathbb{R}^n)$  the set of all such functions with finite norms  $\|\cdot\|_\infty$ .
- A continuous function  $\alpha : \mathbb{R}_+ \rightarrow \mathbb{R}_+$  belongs to the class  $\mathcal{K}$  if  $\alpha(0) = 0$  and the function is strictly increasing;  $\alpha$  belongs to the class  $\mathcal{K}_\infty$  if it is increasing to infinity. A function  $\beta : \mathbb{R}_+ \times \mathbb{R}_+ \rightarrow \mathbb{R}_+$  belongs to the class  $\mathcal{KL}$  if  $\beta(\cdot, t) \in \mathcal{K}$  for each fixed  $t \in \mathbb{R}_+$  and  $\beta(s, \cdot)$  is decreasing and  $\lim_{t \rightarrow \infty} \beta(s, t) = 0$  for each fixed  $s \in \mathbb{R}_+$ . It belongs to the class  $\mathcal{GKL}$  if  $\beta(s, 0) \in \mathcal{K}$ ,  $\beta(s, \cdot)$  is decreasing and for each  $s \in \mathbb{R}_+$  there is  $T_s \in \mathbb{R}_+$  such that  $\beta(s, t) = 0$  for all  $t \geq T_s$ .
- Define the Lambert function  $\mathbf{W} : \mathbb{R} \rightarrow \mathbb{R}$ , as the branches of the inverse relation of the function  $f(z) = ze^z$  for  $z \in \mathbb{R}$ , where  $\mathbf{e} = \exp(1)$ .
- Denote  $\lceil s \rceil^\nu = |s|^\nu \text{sign}(s)$  for any  $s \in \mathbb{R}$  and  $\nu \in \mathbb{R}_+$ .

#### 3.1 Dynamic regressor extension and mixing method

Consider the linear estimation problem:

$$\begin{aligned} x(t) &= \omega^T(t)\theta, & (1) \\ y(t) &= x(t) + w(t), \quad t \in \mathbb{R}, & (2) \end{aligned}$$

where  $x(t) \in \mathbb{R}$  is the model output,  $\theta \in \mathbb{R}^n$  is the vector of unknown constant parameters to be estimated,  $\omega : \mathbb{R} \rightarrow \mathbb{R}^n$  is the regressor function (bounded and known),  $y : \mathbb{R}_+ \rightarrow \mathbb{R}$  is the signal available for measurements and  $w : \mathbb{R} \rightarrow \mathbb{R}$  is the measurement noise.

*Assumption 1.* (Wang et al., 2019) Assume  $\omega \in \mathcal{L}_\infty(\mathbb{R}, \mathbb{R}^n)$  and  $w \in \mathcal{L}_\infty(\mathbb{R}, \mathbb{R})$ .

The DREM procedure (Aranovskiy et al., 2017) transforms (2) into  $n$  new one-dimensional regression models allowing the decoupled estimation of the parameters  $\theta_i$  with  $i = 1, \dots, n$ . For that, first,  $n - 1$  linear operators  $H_j : \mathcal{L}_\infty(\mathbb{R}, \mathbb{R}) \rightarrow \mathcal{L}_\infty(\mathbb{R}, \mathbb{R})$  for  $j = 1, \dots, n - 1$  are introduced. It could be, for example, a stable linear time-invariant operator selected to filter the noise  $w$  or also a delay operator. The application of different linear transformations generates various versions of the original signal  $y \in \mathcal{L}_\infty(\mathbb{R}, \mathbb{R})$ . Therefore, by means of the superposition principle we obtain:  $\tilde{y}_j(t) = H_j(y(t)) = \tilde{\omega}_j^T \theta + \tilde{w}_j(t)$ ,  $j = 1, \dots, n - 1$ ,  $t \in \mathbb{R}_+$ , where  $\tilde{y}_j : \mathbb{R} \rightarrow \mathbb{R}$  is the  $j^{\text{th}}$  linear operator output,  $\tilde{\omega}_j : \mathbb{R} \rightarrow \mathbb{R}^n$  is the  $j^{\text{th}}$  filtered regression function and  $\tilde{w}_j : \mathbb{R} \rightarrow \mathbb{R}$  is the  $j^{\text{th}}$  noise signal composed by the transformation of  $w$  by  $H_j$  and other exponentially converging components due to the initial conditions.

Hence, a new vector of variables

$$\tilde{Y}(t) = [y(t) \tilde{y}_1(t) \dots \tilde{y}_{n-1}(t)] \in \mathbb{R}^n,$$

$$\tilde{W}(t) = [w(t) \tilde{w}_1(t) \dots \tilde{w}_{n-1}(t)] \in \mathbb{R}^n,$$

and a time-varying matrix

$$M(t) = [\omega(t) \tilde{\omega}_1(t) \dots \tilde{\omega}_{n-1}(t)]^T \in \mathbb{R}^{n \times n},$$

are constructed to obtain the extended regressor system

$$\tilde{Y}(t) = M(t)\theta + \tilde{W}(t), \quad t \in \mathbb{R}. \quad (3)$$

It is known that for any matrix  $M(t) \in \mathbb{R}^{n \times n}$ , it holds  $\text{adj}(M(t))M(t) = \det(M(t))I_n$  where  $I_n$  denotes the identity matrix and  $\text{adj}$  the adjoint matrix. Then, by multiplying the both sides of (3) by  $\text{adj}(M(t))$  and defining  $Y(t) = \text{adj}(M(t))\tilde{Y}(t)$ ,  $W(t) = \text{adj}(M(t))\tilde{W}(t)$ , and  $\phi(t) = \det(M(t))$  we finally obtain  $n$  scalar regressor models of the form

$$Y_i(t) = \phi(t)\theta_i + W_i(t), \quad i = 1, \dots, n. \quad (4)$$

By construction,  $Y \in \mathcal{L}_\infty(\mathbb{R}, \mathbb{R}^n)$ ,  $W \in \mathcal{L}_\infty(\mathbb{R}, \mathbb{R}^n)$  and  $\phi \in \mathcal{L}_\infty(\mathbb{R}, \mathbb{R})$ . For the decoupled system (4) different estimation algorithms can be applied.

#### 3.2 Stability notions

Consider a time-dependent differential equation

$$\dot{x}(t) = f(t, x(t), d(t)), \quad t \geq t_0, \quad t_0 \in \mathbb{R} \quad (5)$$

where  $x(t) \in \mathbb{R}^n$  is the state vector,  $d(t) \in \mathbb{R}^m$  is the vector of external inputs,  $d \in \mathcal{L}_\infty(\mathbb{R}, \mathbb{R}^m)$ ,  $f : \mathbb{R}^{n+m+1} \rightarrow \mathbb{R}^n$  is a continuous function with respect to  $x$  and  $d$ , piecewise continuous with respect to  $t$ , and  $f(t, 0, 0) = 0$  for all  $t \in \mathbb{R}$ . Denote by  $X(t, t_0, x_0, d)$  a solution of this system, where  $x(t_0) = x_0 \in \mathbb{R}^n$  is the initial condition at the initial time  $t_0 \in \mathbb{R}$ , and assume that  $X(t, t_0, x_0, d)$  is defined and unique in forward time at least on some finite interval  $[t_0, t_0 + T)$ , where  $T > 0$  may depend on  $x_0$ ,  $d$ , and  $t_0$ .

*Definition 1.* (Wang et al., 2019) The system (5) with  $d \equiv 0$  is *short-fixed-time stable* for  $T^0 > 0$  and  $T_f > 0$  if for any bounded set  $\Omega \subset \mathbb{R}^n$  containing the origin there exists  $\beta \in \mathcal{GKL}$  such that for all  $x_0 \in \Omega$  and  $t_0 \in [-T^0, T^0]$ :

$$|X(t, t_0, x_0, 0)| \leq \beta(|x_0|, t - t_0),$$

for all  $t \in [t_0, t_0 + T_f]$ , and  $\beta(|x_0|, T_f) = 0$ .

By using class  $\mathcal{K}$  and  $\mathcal{GKL}$  functions a robust stability notion of short-fixed-time stability is defined as follows.

*Definition 2.* (Wang et al., 2019) The system (5) is *short-fixed-time ISS* for  $T^0 > 0$  and  $T_f > 0$ , if there exist  $\beta \in \mathcal{GKL}$  and  $\gamma \in \mathcal{K}$  such that for all  $x_0 \in \mathbb{R}^n$ , for all  $d \in \mathcal{L}_\infty(\mathbb{R}, \mathbb{R}^m)$  and  $t_0 \in [-T^0, T^0]$ :

$$|X(t, t_0, x_0, u)| \leq \beta(|x_0|, t - t_0) + \gamma(\|d\|_\infty),$$

for all  $t \in [t_0, t_0 + T_f]$ , and  $\beta(|x_0|, T_f) = 0$ .

#### 3.3 Fixed-time parameter estimation

Now, recover the linear regression model (1), (2) under Assumption 1 and assume that the DREM method has been applied to reduce the initial vector estimation problem to  $n$  one-dimensional regressor models. Since the problem is decoupled on  $n$  independent ones, to simplify the notation, we will omit the index  $i$  by assuming  $n = 1$ :

$$Y(t) = \phi(t)\theta + W(t), \quad (6)$$

where  $\theta \in \mathbb{R}$ ,  $Y \in \mathcal{L}_\infty(\mathbb{R}, \mathbb{R})$ , and  $W \in \mathcal{L}_\infty(\mathbb{R}, \mathbb{R})$ . Two adaptive estimation algorithms generating an estimate

$\hat{\theta}(t) \in \mathbb{R}^n$  of the unknown parameters  $\theta \in \mathbb{R}^n$  have been proposed in Ríos et al. (2017, 2018) and Wang et al. (2019). Such algorithms, according with the following propositions, provide the short-fixed-time stability of the estimation error  $e(t) = \theta - \hat{\theta}(t)$  dynamics given some  $T^0$  and  $T_f$  when  $\|W\|_\infty = 0$ , and short-fixed-time ISS property when  $\|W\|_\infty \neq 0$ .

*Algorithm 1.* (Ríos et al., 2017, 2018)

$$\dot{\hat{\theta}}(t) = \phi(t) \left( \gamma_1 [Y(t) - \phi(t)\hat{\theta}(t)]^{1-\alpha} + \gamma_2 [Y(t) - \phi(t)\hat{\theta}(t)]^{1+\alpha} \right)$$

for  $\gamma_1 > 0$ ,  $\gamma_2 > 0$ , and  $\alpha \in [0, 1)$ , with  $\hat{\theta}(t_0) \in \mathbb{R}$ .

*Proposition 1.* Let Assumption 1 hold. If there exists  $v > 0$  such that for given  $T^0 > 0$  and  $T_f > 0$ ,

$$\int_t^{t+\ell} \min |\phi(s)|^{2-\alpha}, |\phi(s)|^{2+\alpha} ds \geq v > 0 \quad (7)$$

for all  $t \in [-T^0, T^0 + T_f]$  and some  $\ell \in (0, \frac{T_f}{2})$ . Take

$\min\{\gamma_1, \gamma_2\} > \frac{2^{2+\frac{\alpha}{2}}}{\alpha v (\frac{T_f}{2} - 1)}$ , then the estimation error  $e(t) =$

$\theta - \hat{\theta}(t)$  dynamics of (1),

$$\dot{e}(t) = -\phi(t) \left( \gamma_1 [\phi(t)e(t) + W(t)]^{1-\alpha} + \gamma_2 [\phi(t)e(t) + W(t)]^{1+\alpha} \right)$$

is *short-fixed-time ISS* for  $T^0$  and  $T_f$ .

*Algorithm 2.* (Wang et al., 2019)

$$\dot{\hat{\theta}}(t) = \text{sign}(\phi(t)) \left( \gamma_1 [Y(t) - \phi(t)\hat{\theta}(t)]^{\alpha(t)} + \gamma_2 [Y(t) - \phi(t)\hat{\theta}(t)]^{\zeta+\alpha(t)} \right)$$

for  $\gamma_1 > 0$ ,  $\gamma_2 > 0$ ,  $\zeta > 1$ , and  $\alpha(t) = \frac{|\phi(t)|}{1+|\phi(t)|}$ . In this version the power  $\alpha$  is approaching zero together with the regressor  $\phi$ , the contribution of the regressor in the adaptation rate is proportional to  $|\phi(t)|^{\alpha(t)}$ ,  $\forall t \in \mathbb{R}$ .

*Proposition 2.* Let Assumption 1 hold and  $\vartheta \in \mathcal{L}_\infty(\mathbb{R}, \mathbb{R}^n)$  with  $\vartheta(t) = \frac{W(t)}{\phi(t)}$ ,  $\forall t \in \mathbb{R}$ . If there exists  $v > 0$  such that for given  $T^0 > 0$  and  $T_f > 0$ ,

$$\int_t^{t+\ell} |\phi(s)|^\zeta ds \geq v > 0 \quad (8)$$

for all  $t \in [-T^0, T^0 + T_f]$  and some  $\ell \in (0, T_f)$ , and  $\min\{\gamma_1, \gamma_2\} > \sqrt{2} \frac{1+\phi_{\max} + \frac{4\zeta}{(\zeta-1)v}}{(T_f-\ell)g(x_{\min})}$ ,  $\phi_{\max} := \max_{t \in [-T^0, T^0 + T_f]} |\phi(t)|$ ,

$g(x) := x^{\frac{\alpha}{1+\alpha}}$  and  $x_{\min} := \mathbf{W}(e^{-1})$ , then the estimation error  $e(t) = \theta - \hat{\theta}(t)$  dynamics of (2),

$$\dot{e}(t) = -\text{sign}(\phi(t)) \left( \gamma_1 [\phi(t)e(t) + W(t)]^{\alpha(t)} + \gamma_2 [\phi(t)e(t) + W(t)]^{\zeta+\alpha(t)} \right)$$

is *short-fixed-time ISS* for  $T^0$  and  $T_f$  with the input  $\vartheta$ .

The condition (8) can be skipped for (2), then the short-finite-time ISS property can be obtained (the convergence time becomes not uniform in the initial conditions).

#### 4. MAIN RESULTS

According to the data acquisition system characteristics, the sampling frequency of the measured signal is  $0.625Hz$ . By means of analysis of the frequency spectrum of the noise signal (see Fig. 4) it has been found that the main

frequencies are in the range of  $0.02Hz$  to  $0.04Hz$ . Our goal was to suppress these frequencies with minor or none alteration of the basic biological record. However, using conventional lowpass or bandstop filters, we observed that important components of the original signal were also suppressed or that high frequency measurement noise was maintained. These results will be presented later for comparison in the simulation section.

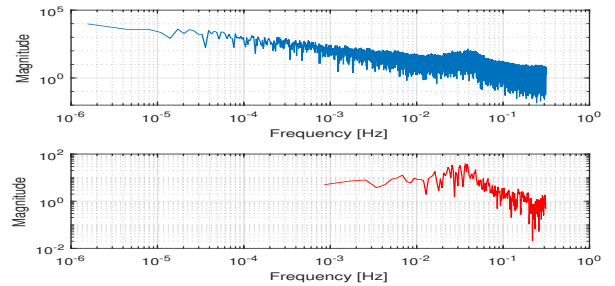


Fig. 4. The frequency spectrum of the distance signal measured from the animal #1 (up) and the frequency spectrum of the electronic noise signal (down)

To solve this problem we propose an adaptive filter, robust and/or tolerant to electrical and measuring noises, able to maintain the relevant information from the original signal even if the unwanted components are in the same frequency range. In our specific problem, a model for the original signal can be chosen as

$$y(t) = d(t) + f(t) + w(t), \forall t \in \mathbb{R}$$

where  $d$  is the filtered signal,  $f$  is the fault signal and  $w$  is the measurement noise. Since the fault resembles a sinusoidal signal, we can approximate it by the function

$$f(t) = a(t) \sin(\omega_0 t + \varphi), \forall t \in \mathbb{R}$$

where  $a$  is the amplitude,  $\omega_0$  is the nominal frequency, and  $\varphi$  is the phase shift. Hence, we obtain for the nominal model the following equation

$$y(t) = d_0 + a_0 \cos(\varphi) \sin(\omega_0 t) + a_0 \sin(\varphi) \cos(\omega_0 t) + w(t), \forall t \in \mathbb{R}.$$

*Remark 1.* Other frequency components could be added to the model. But increasing the model structure also increases the number of parameters to be estimated. Therefore, it should be assessed whether the new component added has a significant influence on the filtered signal.

Assuming  $\theta_1 = a_0 \cos(\varphi)$ ,  $\theta_2 = a_0 \sin(\varphi)$ , and  $\theta_3 = d_0$ , we can rewrite the filter problem as a linear regression one in the form of Eq. 2:

$$y(t) = \omega(t)^T \theta + w(t), \quad \omega(t) = \begin{bmatrix} \sin(\omega_0 t) \\ \cos(\omega_0 t) \\ 1 \end{bmatrix}. \quad (9)$$

In this case, the filtered signal results from the estimates of  $\theta_3$ , i.e. a time-dependent parameter which varies relatively slowly in time. In such a model,  $\theta_1$  and  $\theta_2$  are proportional to the oscillation amplitude  $a_0$  and vary much faster. We consider the nominal frequency as the average frequency of the electrical noise, thus  $\omega_0 \approx 0.1885rad/s$ .

As we can see, we need to estimate  $n = 3$  parameters, under the constraint that  $\theta_3$  varies slowly, while  $\theta_1$  and  $\theta_2$  admit fast changes, so these features have to be retained

in the adaptation algorithm. Therefore, we need an estimation approach that allows such a decomposition and control on the velocity of adjustment, and DREM is an example of this kind of method.

*Remark 2.* The proposed approach takes place in two separate steps. The first step is to decompose the nominal model so that its parameters are estimated independently. The second step is to adaptively estimate these parameters during a small fixed window of time. Therefore, at this stage, we assume that these parameters are slowly varying, and in the time window of estimation they stay constant. That is, they can suddenly change the values when the noise appears, being constant meanwhile.

To apply the DREM method we choose  $n - 1$  linear operators  $H_j : \mathcal{L}_\infty(\mathbb{R}, \mathbb{R}) \rightarrow \mathcal{L}_\infty(\mathbb{R}, \mathbb{R})$ . The first one is a stable linear time-invariant first order filter with transfer function  $G_1(s) = \frac{\lambda}{s+\lambda}$ , where  $s \in \mathbb{C}$  is a complex variable and  $\lambda > 0$  is selected to filter the noise  $w$  in (9). The second one is a delay operator with transfer function  $G_2(s) = e^{-\tau s}$  for  $\tau > 0$ . According with the signal characteristics we can choose  $\lambda$ , for example, to realize a first-order lowpass filter with cutoff frequency  $\omega_c$  smaller than  $\omega_0$  (in this way the high-frequency components, including the electrical and the measurement noises, will be suppressed). The time-delay can be chosen as a fraction of the sample time  $T_s = 1.6s$  ( $\tau = T_s \delta$  with decimation constant  $\delta > 1$ ). Finally, once different versions of  $y$  and  $\omega$  are generated we rewrite the model (9) in the form (4):

$$Y_i(t) = \phi(t)\theta_i + W_i, \quad i = 1, \dots, 3. \quad (10)$$

and apply the algorithm 1 or 2 to dissociate the desired filtered signal given by the parameter  $\theta_3$ . Applying the algorithm 1, for example, we have to tune the parameters  $\gamma_1, \gamma_2$  and  $\alpha_1$  to estimate  $\theta_1$ ;  $\gamma_3, \gamma_4$  and  $\alpha_2$  to estimate  $\theta_2$ ; and  $\gamma_5, \gamma_6$ , and  $\alpha_3$  to estimate  $\theta_3$ . For (9) there is no  $\alpha_i$ , but the parameters  $\zeta_i$  appear for  $i = 1, 2, 3$ .

#### 4.1 Filter parameter tuning

Different techniques can be used to choose the parameters  $\gamma$ 's,  $\alpha$ 's and  $\zeta$ 's. In this work, we used a simple grid search procedure, *i.e.* we vary each parameter in a range of values and validate the error between the measured signal and the estimated signal. In this case the normalized root means square error (NRMSE) was used:

$$\text{NRMSE} = 100 \times \left( 1 - \frac{\sqrt{\sum_{k=1}^N (y(k) - \hat{y}(k))^2}}{\sqrt{\sum_{k=1}^N (y(k) - \bar{y})^2}} \right),$$

where  $y$  is the measured signal,  $\hat{y}$  is the estimated signal,  $\bar{y}$  is the average of the data window, taken as a reference to compare filter performance,  $N$  is the window size, and  $k$  is the available sample. The closer is NRMSE to 100% the better the estimation fits the measured data.

To determine comparisons it is necessary to have a reference signal. To generate this reference we used a signal measured from another animal in another year which does not contain the electrical noise. An example of this kind of signal is shown in Fig. 5 (up). Then we added artificially a sinusoidal signal in the shape of the electric fault (see Fig. 5 (down)) resulting in a signal with noise. Hence, by means of the proposed filters we recover from the signal

artificially corrupted, the signal without noise. Finally, when we reach the estimation with the smallest error the estimator parameters are set. Following this procedure we found the values indicated on Table 1. Note that the NRMSE index was calculated by comparing the measured signal  $y(k) = \theta_3(k)$  with the filtered signal  $\hat{y}(k) = \hat{\theta}_3(k)$ .

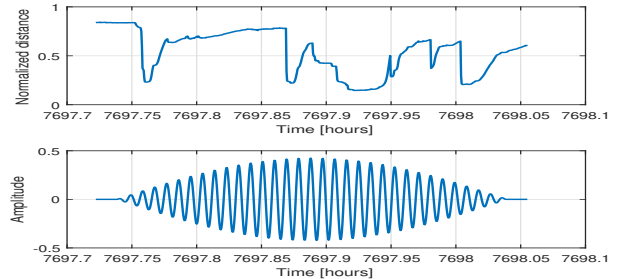


Fig. 5. Reference signal (up) measured from animal #10 in 2016 and noise signal (down) artificially added for tuning process

Table 1. Estimator parameters.

Algorithm 1		
Parameter	Value	NRMSE (%)
$\gamma_1 = \gamma_2 = \gamma_3 = \gamma_4$	50	70.65
$\alpha_1 = \alpha_2$	0.1	
$\gamma_5 = \gamma_6$	70	
$\alpha_3$	0.3	
Algorithm 2		
$\gamma_1 = \gamma_2 = \gamma_3 = \gamma_4$	10	70.65
$\zeta_1 = \zeta_2$	1.25	
$\gamma_5 = \gamma_6$	10	
$\zeta_3$	1.25	

#### 4.2 Filter performance comparison

To evaluate the performance of adaptive filters, we compared the obtained results with two conventional approaches. The first one is a Butterworth bandstop filter that is designed to suppress the frequencies between  $0.02Hz$  and  $0.04Hz$ , which constitute the range of the main components of the electronic noise. The second one is a lowpass Butterworth filter created to suppress the frequencies above  $0.02Hz$ . In both cases, we use 6th-order filters. The Butterworth approach was chosen being one of the most popular in signal processing practice for its simplicity and effectiveness.

Fig. 6 shows the time domain response of the applied bandstop filter to the distance signal from the animal #1 in a sampling window containing the measured signals from the day 321.48 to 321.58. This data window was chosen since it contains three main regions typically found in the measured distance signals of the scallops that include a high frequency but low amplitude region (I), a low frequency but wide amplitude region (II), and the region affected by the electronic noise (III). Note that by using the bandstop filter there exists an attenuation in the amplitude of the signal in the region III and the filtered signal follows well the behavior in the region II. However, in the region I, by the figure detail, it is possible to see that some high-frequency behavior is kept.

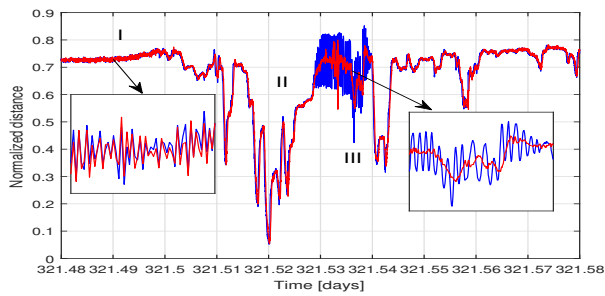


Fig. 6. Distance measured for animal #1 from day 321.48 to 321.58 in 2017 (blue), filtered by a Butterworth lowpass filter (red)

Assuming that the effect in region *I* is due to measurement noise, a smoother response would be desired, so an appropriate solution would be to filter the frequencies above  $0.02\text{Hz}$ . In this case, a Butterworth lowpass filter was designed. The temporal response of this filter is shown in Fig. 7. In this case, the signal was more attenuated in region *I*. In addition, the amplitude of the signal was maintained in the region *II*. However, some oscillations remains in region *III*. With these two approaches, we illustrate the problem that arises when unwanted frequency components are in the same frequency range as the important frequencies of the original signal (see Fig. 4).

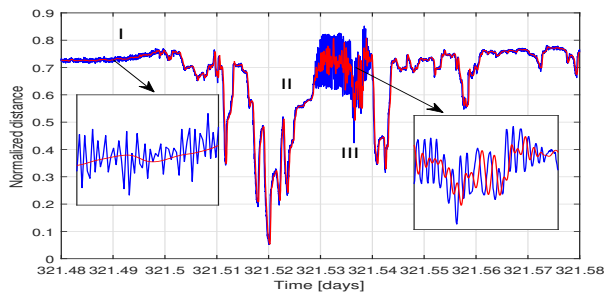


Fig. 7. Distance measured for animal #1 from day 321.48 to 321.58 in 2017 (blue), filtered by a Butterworth bandstop filter (red)

Finally, the results obtained using the algorithms (1) and (2) are shown, respectively, in Figs. 8 and 9. By proposing a model for the original signal, including a model for the faulty component, and identifying its parameters, it was possible to remove from the original signal the electrical noise. Moreover, due to the greater freedom in parameter set-up, it was also possible to reduce the effect of the measurement noise. Note that the filtered signal keeps the same characteristics, in terms of frequency, on the three highlighted regions. The performance of both algorithms is similar. A technical difference between the two algorithms is that the algorithm (2) has more sensitivity to measurement noise and conversely the algorithm (1) has lower mean error and less error oscillation.

## 5. CONCLUSION

In this paper, a model-based adaptive filter was designed to suppress electrical noise in a high-frequency noninvasive valvometry system. For that, it was proposed a structure for the valve opening/closing activity signals of scallops *Chlamys islandica*. Such a structure includes a model for the electrical noise which was considered as a failure. The

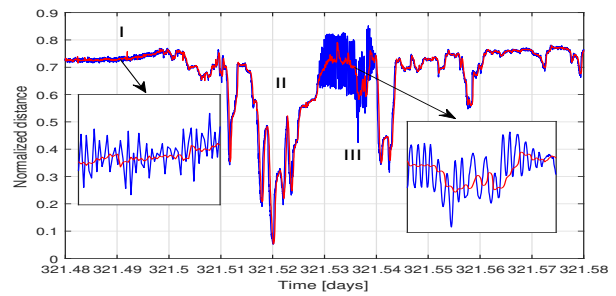


Fig. 8. Distance measured for animal #1 from day 321.48 to 321.58 in 2017 (blue), filtered by algorithm 1 (red).

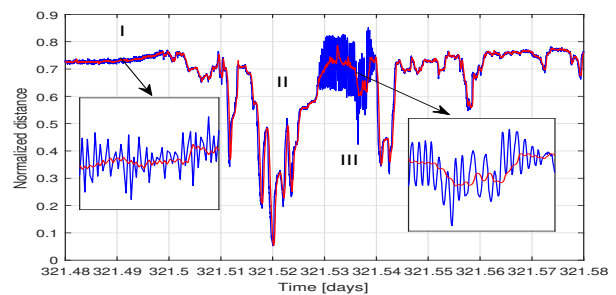


Fig. 9. Distance measured for animal #1 from day 321.48 to 321.58 in 2017 (blue), filtered by algorithm 2 (red).

design of the filters was based on the dynamic regressor extension and mixing method, which allows the parameters to be decoupled for estimation (hence, the speed of convergence and adjustment for each parameter can be regulated separately). Once the desired regression form of the proposed output model was obtained, different fixed-time estimation approaches were used to identify its parameters. By applying these two techniques, a flexible filter structure was obtained. The results showed that by using the adaptive filters it was possible to retain the major relevant components of interest of the original valve-activity signals, even if the unwanted signal frequency components belong to the frequency range of valve-activity.

## REFERENCES

- Andrade, H., Massabuau, J.C., Cochrane, S., Ciret, P., Tran, D., Sow, M., and Camus, L. (2016). High frequency non-invasive (HFNI) bio-sensors as a potential tool for marine monitoring and assessments. *Frontiers in Marine Science*, 3. doi:<https://doi.org/10.3389/fmars.2016.00187>.
- Aranovskiy, S., Bobtsov, A., Ortega, R., and Pyrkin, A. (2017). Performance enhancement of parameter estimators via dynamic regressor extension and mixing. *IEEE Transactions on Automatic Control*, 62, 3546–3550.
- Gao, Z., Cecati, C., and Ding, S.X. (2015). A survey of fault diagnosis and fault-tolerant techniques, parts I, II: Fault diagnosis with model-based and signal-based approaches. *IEEE Trans. on Industrial Electronics*, 62.
- Lathi, B.P. (2009). *Signal Processing and Linear Systems*. Oxford University Press, Oxford.
- Ljung, L. (1999). *System Identification Theory for the User*. Prentice Hall, New Jersey.
- Lutavac, M.D., Toi, D.V., and Evans, B.L. (2000). *Filter Design for Signal Processing Using MATLAB and Mathematica*. Prentice Hall, New Jersey.
- Pintelon, R. and Schoukens, J. (2012). *System Identification A Frequency Domain Approach*. Wiley-IEEE Press, New Jersey.
- Ríos, H., Efimov, D., Moreno, J.A., Perruquetti, W., and Rueda-Escobedo, J.G. (2017). Time-varying parameter identification algorithms: Finite and fixed-time convergence. *IEEE Transactions on Automatic Control*, 62, 3670–3678.
- Ríos, H., Efimov, D., and Perruquetti, W. (2018). An adaptive sliding-mode observer for a class of uncertain nonlinear systems. *International Journal of Adaptive Control and Signal Processing*, 32, 3670–3678.
- Wang, J., Efimov, D., Aranovskiy, S., and Bobtsov, A. (2019). Fixed-time estimation of parameters for non-persistent excitation. *European Journal of Control*.
- Widrow, B. and Stearns, S.D. (1985). *Adaptive Signal Processing*. Prentice Hall, New Jersey.